Transfer-Matrix Analysis of Optical Bistability in DFB Semiconductor Laser Amplifiers with Nonuniform Gratings

Drew N. Maywar and Govind P. Agrawal, *Fellow, IEEE*

***Abstract*— We present a transfer-matrix method capable of simulating the effects of nonuniform gratings on the filtering, amplification, and bistability characteristics of distributed feedback (DFB) semiconductor laser amplifiers. The linewidth enhancement factor is incorporated in a way that allows direct gain-tuning of the bistability hysteresis. As an example, we compare a $\lambda/4$ phase-shifted DFB amplifier with and without spatial chirp. For amplifiers driven to yield the same unsaturated peak amplifier gain, positive linear chirp widens the spectral range of low-threshold switching and increases the switching contrast.**

***Index Terms*— Amplifiers, coupled-mode analysis, distributed feedback devices, gratings, optical bistability, optical logic devices.**

I. Introduction

INTEREST in utilizing optical bistability of semiconductor laser amplifiers (SLA's) for photonic switching and optical memory applications has flourished in part because of the development of semiconductor technology and its potential for large-scale integration. Moreover, SLA's exhibit exceptional bistability characteristics such as low (microwatt) switching powers, fast (nanosecond) switching speeds, inherent optical gain, and wavelength compatibility with optical communication systems [1]. Researchers have utilized optical bistability in SLA's for optical logic (e.g., optical AND gate [2], optical memory [3], and optical flip-flop [4]) and optical signal processing (e.g., optical signal regenerator [5] and optical cross-bar switching [6]). Since each application may have unique requirements in terms of the amplifier's bistability hysteresis, it is advantageous to have a means of tailoring the bistability characteristics to fit the application.

For distributed feedback (DFB) devices making use of a built-in grating, one way of tailoring the general transmission behavior is by introducing nonuniformities into the periodic structure [7]. Such nonuniformities include spatial frequency chirp, amplitude taper, and abrupt phase shifts of the grating corrugation. To simulate the effects of these nonuniformities on the transmission spectra of DFB devices with moderate grating depth, it is common to use a transfer-matrix method (TMM) based on the counterpropagating coupled-mode equations [8]–[14]. The TMM can simulate structures with complicated grating nonuniformities while retaining physically intuitive parameters and remaining computationally inexpensive (2×2 matrix multiplication). For these reasons, we want to use the TMM to study the effects of grating nonuniformities on optical bistability in DFB SLA's.

The standard implementation of the TMM [8] for amplifiers with nonuniform gratings is not, in general, appropriate for bistability in semiconductor amplifiers because it fails to take into account gain saturation and the strong coupling that exists between changes in gain and the refractive index. These processes give rise to an intensity-dependent refractive index that is about three orders of magnitude larger than that resulting from the third-order susceptibility (the Kerr effect) of the semiconductor. The combination of this intensity-dependent refractive index and distributed feedback leads to regions of optical bistability.

Optical bistability in DFB SLA's has been theoretically studied for amplifiers with uniform gratings, where an average intensity distribution was (appropriately) used [15]–[17]. Grating nonuniformities, however, cause the intensity distribution to vary significantly within a DFB device. For example, phase-shifted devices exhibit a strong localization of internal intensity near the grating phase shift [12]. The nonuniform intensity distribution resulting from grating nonuniformities influences the bistability characteristics of the amplifiers and requires a better approximation.

The object of this paper is to present a TMM capable of simulating optical bistability in DFB SLA's with nonuniform gratings. In Section II, we incorporate within the transfer matrix the effects of gain saturation and the coupling between the gain and the refractive index that exists in active semiconductors. In Section III, we show by including this coupling how the small-signal amplification characteristics are affected by grating nonuniformities. In Section IV, we use the internal-intensity distribution provided by the TMM itself to calculate the gain-saturation-induced optical bistability for nonuniform amplifiers. Throughout this paper, the computational results are presented for linearly chirped, $\lambda/4$-phase-shifted DFB SLA's with emphasis on improvements realized by the use of these nonuniformities. Examples of such improvements include a wider spectral range of low-threshold switching and a higher on–off switching contrast.

II. Transfer Matrix for Active Semiconductors

A single transfer matrix is used to transfer, or propagate, an optical field through a uniform DFB structure, as depicted

Manuscript received March 5, 1997; revised July 3, 1997. This work was supported in part by the U.S. Department of Education.

The authors are with The Institute of Optics, University of Rochester, Rochester, NY 14627 USA.

Publisher Item Identifier S 0018-9197(97)07809-3.

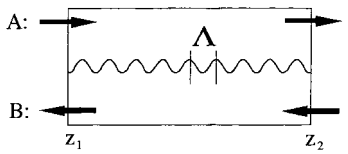

(a)

$$\begin{pmatrix} A(z_2) \\ B(z_2) \end{pmatrix} = \begin{bmatrix} t_{11} & t_{12} \\ t_{21} & t_{22} \end{bmatrix} \begin{pmatrix} A(z_1) \\ B(z_1) \end{pmatrix}$$

(b)

Fig. 1. (a) Uniform DFB structure of grating period Λ. The parameters A and B are the slowly varying forward- and backward-propagating fields, respectively, and (b) the corresponding transfer-matrix representation of propagation through the uniform DFB structure.

in Fig. 1. The quantities $A(z)$ and $B(z)$ in Fig. 1(a) are the slowly varying amplitudes of the forward- and backward-propagating fields, respectively. They are related to the optical field via

$$\tilde{E}(x, y, z, t) = \mathrm{Re}\{\hat{\varepsilon}F(x, y)[A(z)\exp(i\beta_o z) + B(z)\exp(-i\beta_o z)]\exp(-i\omega_o t)\} \quad (1)$$

where $\mathrm{Re}\{\}$ stands for the real part, $\hat{\varepsilon}$ is the unit vector along the direction of polarization, $F(x, y)$ is the transverse modal distribution of the fundamental mode supported by the active waveguide, and ω_o is the optical frequency. The Bragg wavenumber β_o is related to the period Λ of the (first-order) grating by

$$\beta_o = \frac{\pi}{\Lambda}. \quad (2)$$

By using (1) together with a periodic form of the dielectric function in Maxwell's equations, the slowly varying amplitudes $A(z)$ and $B(z)$ are found to satisfy the following coupled-mode equations [18], [19]:

$$\frac{dA}{dz} = i\Delta\beta A + i\kappa B \quad (3a)$$

$$\frac{dB}{dz} = -i\Delta\beta B - i\kappa A \quad (3b)$$

where $\Delta\beta = \beta - \beta_o$ is the detuning of the wavenumber β from the Bragg wavenumber and κ is the coupling coefficient representing the strength of the coupling between the counter-propagating fields. We simplify our discussion to a κ that is due to an index grating and assume that κ is a real constant (we refer the reader to [20] for a more general form of κ). Also, we neglect amplifier noise, assuming that the input field is much stronger than the amplified spontaneous emission [21].

For constant parameters, the coupled-mode equations can be solved analytically, and the solutions can be used to construct a transfer matrix [8], [14]. The matrix elements [see Fig. 1(b)] are given by

$$t_{11} = \frac{1}{1-r^2}\left[e^{iq\ell} - r^2 e^{-iq\ell}\right] \quad (4a)$$

$$t_{21} = -t_{12} = \frac{r}{1-r^2}\left[e^{iq\ell} - e^{-iq\ell}\right] \quad (4b)$$

$$t_{22} = \frac{1}{1-r^2}\left[e^{-iq\ell} - r^2 e^{iq\ell}\right] \quad (4c)$$

where ℓ is the length of the uniform DFB structure. The parameter r represents the effective reflectivity due to the distributed feedback and is given by [19]

$$r = \frac{-\kappa}{q + \Delta\beta} = \frac{q - \Delta\beta}{\kappa}. \quad (5)$$

The parameter q is given by

$$q = \pm\sqrt{\Delta\beta^2 - \kappa^2} \quad (6)$$

with the sign of q chosen such that $|r| \leq 1$. Since the product of $q\ell$ appears in (4), it is convenient to use the dimensionless parameters $\kappa\ell$ and $\Delta\beta\ell$.

The use of the TMM for amplifiers requires that gain be included in the expression for $\Delta\beta$. For nonsemiconductor amplifiers, this parameter is commonly expressed as

$$\Delta\beta = \delta - i\frac{g}{2} \quad (7)$$

where g is the modal power gain and δ is the detuning given as

$$\delta = \frac{2\pi n_o}{\lambda_o} - \frac{\pi}{\Lambda}. \quad (8)$$

The parameter n_o is the real part of the spatially averaged refractive index. The free-space wavelength λ_o is related to the optical frequency ω_o by $\lambda_o = 2\pi c/\omega_o$, where c is the speed of light in vacuum.

For *semiconductor* laser amplifiers, a more appropriate form of $\Delta\beta$ is given as

$$\Delta\beta = \delta - i\frac{g}{2}(1 - i\alpha) + i\frac{\alpha_{\mathrm{int}}}{2} \quad (9)$$

where α_{int} is the internal loss mainly due to scattering and free-carrier absorption [19]. The gain g for semiconductors is typically expressed as

$$g = \Gamma a(N - N_o) \quad (10)$$

where a is the differential gain parameter, N is the charge-carrier density, N_o is the carrier density at transparency, and Γ is the optical confinement factor representing the fraction of the optical mode power contained within the active region. Equation (8) can also be used for SLA's if we interpret n_o as the real part of the spatially averaged modal refractive index at transparency ($N = N_o$). The parameter α is the linewidth enhancement factor and governs the change in the refractive index through variations in the carrier density [19]. It should be noted that although several parameters such as α and α_{int} depend on the wavelength, they vary little over a wavelength scale comparable to the stop band of the grating. Also, although (10) is valid only at the gain peak, this functional form varies little over the stop band. Therefore, we neglect the wavelength dependence of these parameters in our analysis.

The carrier density can be obtained by solving the rate equation [19]

$$\frac{dN}{dt} = \frac{J}{ed} - \frac{N}{\tau_c} - \frac{g}{\hbar\omega_o} I \quad (11)$$

where J is the current density in the active region of thickness d, e is the electron charge, τ_c is the carrier lifetime, $\hbar\omega_o$ is the

photon energy, and I is the optical intensity. We assume that the incident signal is either time-independent (CW signal) or pulsed such that the pulsewidth is much larger than the carrier lifetime τ_c. In that case, the carrier density reaches a steady state with the value

$$N = \frac{\overline{J} + \overline{I}}{1 + \overline{I}} N_o \tag{12}$$

where $\overline{I} = I/I_{\text{sat}}$ is the optical intensity normalized to the saturation intensity $I_{\text{sat}} = \hbar\omega_o/\Gamma a\tau_c$, and $\overline{J} = J/J_o$ is the current density normalized to its value required to achieve transparency $J_o = edN_o/\tau_c$. Substituting (12) into (10) gives the following expression for the power gain:

$$g = \frac{g_o}{1 + \overline{I}} \tag{13}$$

where $g_o = \Gamma a N_o(\overline{J} - 1)$ is the unsaturated value of g. If needed, one can relate the saturation intensity to the saturation power by $P_{\text{sat}} = I_{\text{sat}} W d$, where W is the width of the active region.

In solving (11), we neglected carrier diffusion by assuming that its effect is to average any variations in carrier density which occur over distances smaller than the diffusion length ($\sim$2 μm). For this same reason, the optical intensity $\overline{I}$ in (13) can be represented as

$$\overline{I}(z) = \frac{|A(z)|^2 + |B(z)|^2}{I_{\text{sat}}}. \tag{14}$$

The neglected interference terms burn spatial holes in the carrier density with a period that is much smaller than the diffusion length. We assume that carrier diffusion washes out these holes and produces a carrier density that is uniform over a few optical cycles.

III. Small-Signal Amplification

In this section, we study how the small-signal filtering and amplification characteristics of DFB SLA's are affected by nonuniform gratings. Since gain saturation can be neglected, all device characteristics become intensity-independent in this linear regime. To take into account nonuniformities, we consider the amplifier of length L as being composed of several uniform subsections of length ℓ [8]. Each subsection can therefore be represented mathematically by a transfer matrix of the type described in Section II. The product of all transfer matrices yields a total transfer matrix which characterizes propagation through the entire amplifier. Although we neglect facet reflections throughout this paper, nonzero facet reflectivities can be included in a straightforward manner [14], [17].

To incorporate grating-phase shifts, a matrix designed to shift the phase of the optical field is inserted between two transfer matrices corresponding to uniform subsections on each side of the phase shift [11]. As an example, consider a $\lambda/4$ phase-shifted DFB amplifier. The total transfer matrix of this device can be written as

$$\begin{bmatrix} t_{11} & t_{12} \\ t_{21} & t_{22} \end{bmatrix} \begin{bmatrix} \exp(i\pi/2) & 0 \\ 0 & \exp(-i\pi/2) \end{bmatrix} \begin{bmatrix} t_{11} & t_{12} \\ t_{21} & t_{22} \end{bmatrix}$$

where $\pi/2$ is the phase shift experienced by the field at the center of the amplifier. The transfer-matrix elements are obtained from (4) by using $\ell = L/2$.

Before considering a semiconductor DFB amplifier, it is instructive to discuss results for a nonsemiconductor device for which $\alpha = 0$. The wavelength dependence of the amplifier gain $G(G = I_{\text{out}}/I_{\text{in}})$ of a $\lambda/4$ phase-shifted DFB nonsemiconductor amplifier is shown in Fig. 2(a). For this device, we have chosen $\kappa L = 3$ and $\alpha_{\text{int}} L = 0$, values that we maintain throughout this paper. The transmission peak centered at $\delta = 0$, caused by the abrupt phase shift in the grating, benefits the most from the distributed feedback; as $g_o L$ is increased (by increasing the pump current), the central transmission peak grows significantly more than any other spectral region. In the figure, we use values of $g_o L$ that yield peak G values of 10, 20, and 30 dB ($g_o L = 0.4360$, 0.5854, and 0.6339, respectively). As a reference, a spectral width of $\delta L = 1$ corresponds to a wavelength band of 0.45 nm (about 60 GHz) for a 250-μm-long DFB amplifier operating near 1.55 μm.

The effect of the linewidth enhancement factor on the transmission spectrum is to produce a shift in the spectrum proportional to the change in gain ($g_o L$). This shift is apparent in Fig. 2(b), where we have used the same values of the device parameters as in Fig. 2(a) except that $\alpha = 5$. The spectral shift is easily understood by noting that an increase in gain for a semiconductor amplifier results in a decrease in the refractive index. Consequently, the transmission spectrum shifts to higher values of δ [see (9)]. The shift between transmission peaks decreases for higher values of G because less increase in $g_o L$ is needed for a 10-dB increase in G [see inset of Fig. 2(b)]. The capability of tuning the transmission peak via direct variation of $g_o L$ (i.e., pump current) enriches the device applications of semiconductor amplifiers. For example, this tunability has been used as the basis for a wavelength-division demultiplexer [22]–[24].

To further exploit the effects of grating nonuniformities, we now consider how the small-signal amplification spectrum is affected by linear spatial chirp. Spatial chirp can be introduced into a grating by several methods such as varying the grating pitch or bending the active waveguide [25], [26]. The Bragg wavenumber β_o is represented by

$$\beta_o(z) = \overline{\beta}_o + C\left(\frac{z - L/2}{L^2}\right) \tag{15}$$

where $\overline{\beta}_o$ is the average value of the Bragg wavenumber and the chirp parameter C is related to the rate at which the grating period varies along the amplifier length. The TMM approximates the continuous variation in the Bragg wavenumber by a step-like distribution and therefore the accuracy of this approximation is improved by increasing the number of subsections. However, the TMM requires that the length of each subsection be chosen such that $\lambda \ll \ell$ [8], and therefore limits the number of subsections for a given device. Nonetheless, in practice we are able to reproduce results for a continuously chirped structure with as few as eight subsections.

As an example of the effect of linear spatial chirp on the transmission spectra of DFB SLA's, we add this nonuniformity

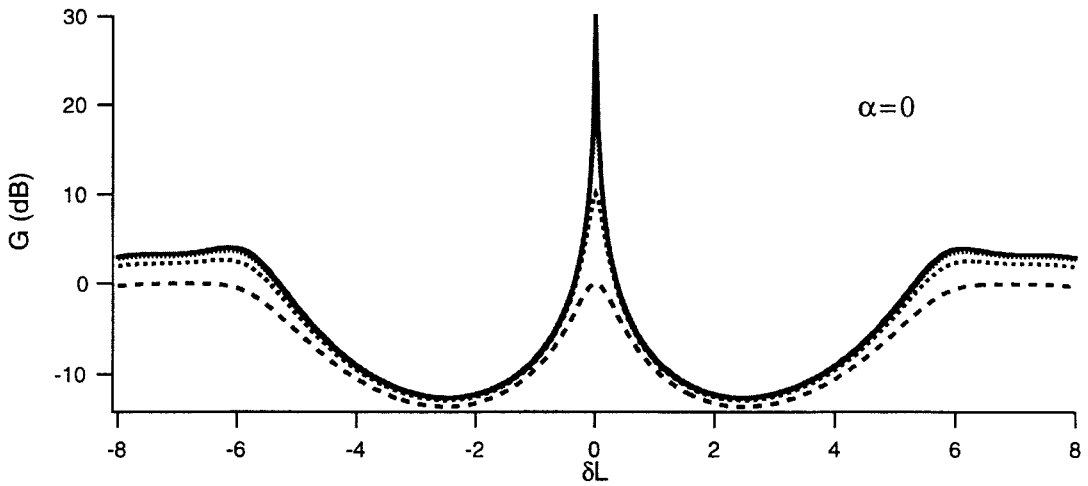

(a)

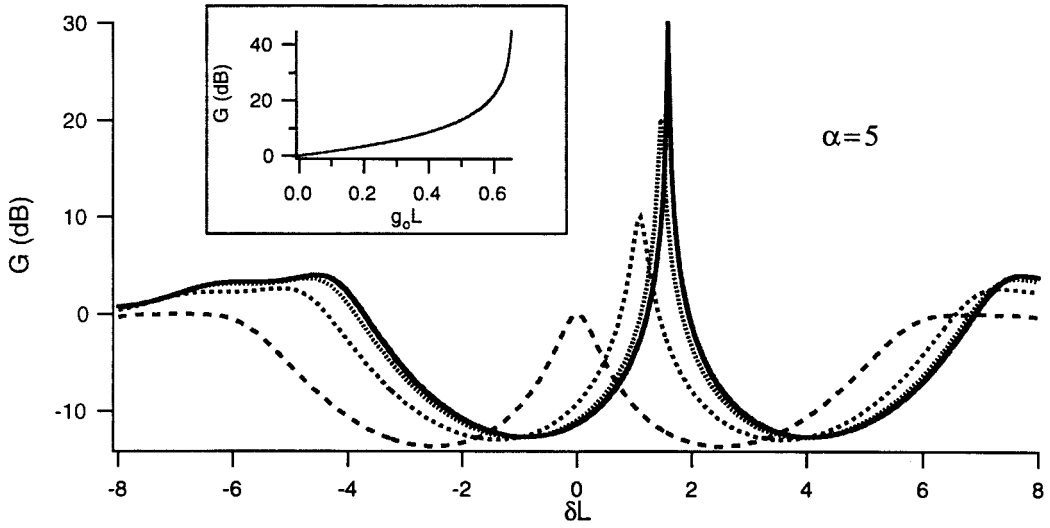

(b)

Fig. 2. (a) Wavelength dependence of the amplifier gain G for a $\lambda/4$ phase-shifted DFB nonsemiconductor amplifier ($\alpha = 0$) with $\kappa L = 3$ and $\alpha_{\rm int} L = 0$, for values of $g_o L$ corresponding to peak G values of 0, 10, 20, and 30 dB. See (8) for the relation between δ and the free-space wavelength and (b) wavelength dependence of the amplifier gain G for a $\lambda/4$ phase-shifted DFB SLA with $\alpha = 5$, $\kappa L = 3$, and $\alpha_{\rm int} L = 0$, for values of $g_o L$ corresponding to peak G values of 0, 10, 20, and 30 dB. Insert shows the value of $g_o L$ required to obtain a certain value of G, where the right-hand-side cut-off corresponds to the lasing threshold of the device.

to the grating of the $\lambda/4$ phase-shifted amplifier considered above. For the unchirped case, the wavelength corresponding to the Bragg wavenumber experiences the greatest feedback and exhibits the most amplifier gain. Feedback for this wavelength, though, is reduced when chirp is introduced because the Bragg condition is satisfied only over a portion of the device.

As a result of lower feedback, higher values of $g_o L$ are required to realize peak G values of 10, 20, and 30 dB ($g_o L = 1.4200$, 2.1912, and 2.4914, respectively). The transmission spectrum is consequently shifted to higher values of δ compared to the case $C = 0$ [Fig. 2(b)]. This effect can be seen in Fig. 3, where we show the wavelength dependence of the amplifier gain G for a linearly chirped, $\lambda/4$ phase-shifted DFB SLA with $C = 20$. The wide transmission peaks of Fig. 3 can be understood as follows. Since the Bragg wavenumber varies along the length of the device, a range of wavelengths experience strong feedback, thereby widening the transmission peak. Thus, spatial chirp allows amplification of (temporally) narrower pulses.

When comparing Figs. 2(b) and 3, note that the corresponding wavelengths can be chosen by varying either the grating pitch Λ or the average refractive index n_o [see (8)]. Thus, the wavelength of any peak from Fig. 3 can be made to coincide with the wavelength of any peak from Fig. 2(b) by considering, for example, devices of two different grating pitches.

However, the spacing (in $g_o L$) between peaks is different for Figs. 2(b) and 3, and this prevents more than one peak from coinciding. For example, if the 30-dB peaks of Figs. 2(b) and 3 are made to coincide to the same wavelength, the 20-, 10- and 0-dB peaks do not coincide. The wider peak spacing for the case of $C = 20$ is a result of the difference between the slopes of G as a function of $g_o L$, as shown in the inset of Fig. 3. It is interesting to note that higher discrimination (i.e.,

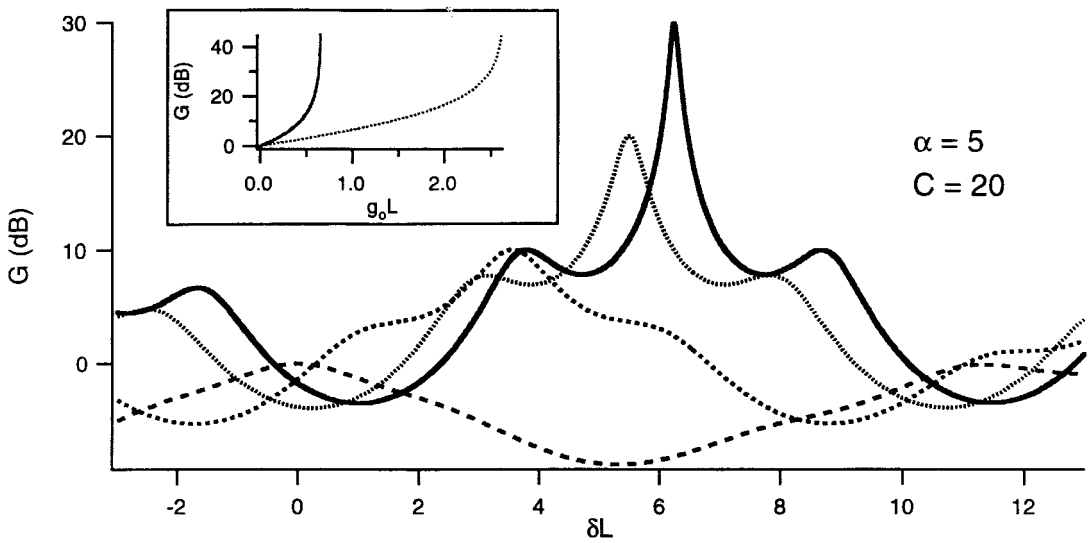

Fig. 3. Wavelength dependence of the amplifier gain G for a linearly chirped, $\lambda/4$ phase-shifted DFB SLA with $C = 20$, $\alpha = 5$, $\kappa L = 3$, and $\alpha_{\rm int} L = 0$, for values of $g_o L$ corresponding to peak G values of 0, 10, 20, and 30 dB. Insert shows the value of $g_o L$ required to obtain a certain value of G for the cases $C = 0$ (left) and $C = 20$ (right).

wider peak separation) exists between adjacent transmission peaks for $C = 20$, even though the peaks are wider than for the case of $C = 0$. Thus, the introduction of linear spatial chirp allows the amplification of narrower pulses *and* may improve discrimination between different channels in wavelength-division demultiplexing applications.

IV. Optical Bistability

All amplifiers are inherently nonlinear because of gain saturation occurring in the large-signal regime. In semiconductor amplifiers, this gain saturation is accompanied by a nonlinear index change. This intensity-dependent refractive index works together with distributed feedback to produce regions of dispersive bistability (originally studied theoretically by Winful *et al.* [27] for Kerr-type nonlinear media). In this section, we study how the optical bistability characteristics of DFB SLA's are affected by nonuniform gratings.

One effect of nonuniformities is to alter the intensity distribution within the amplifier. The optical field distribution is calculated by assuming an initial field at one facet and applying one transfer matrix at a time until the other facet is reached. Each application of a transfer matrix yields a value of the internal field. The corresponding effective optical intensity is computed using (14).

For a $\lambda/4$ phase-shifted DFB SLA, the small-signal intensity distribution of the wavelength that experiences the largest amplifier gain is strongly localized at the location of the phase shift. Detuning away from this wavelength results in the reduction of the intensity peak within the device, as shown in Fig. 4(a). The intensity within the amplifier is further distorted by the incorporation of linear spatial chirp. For $C = 20$, the phase-shift-induced peak of the wavelength with the largest amplifier gain is almost completely flattened, and the intensity near each amplifier facet is higher than that of the center. In addition, the small-signal intensity distribution is asymmetric about the wavelength with the largest amplifier gain. As seen in Fig. 4(b), the short-wavelength side recovers a prominent central peak, whereas the long-wavelength side obtains its lowest value at the center of the amplifier and exhibits higher intensities near both amplifier facets.

The nonuniform intensity profile in an active semiconductor will create a nonuniform gain profile via saturation. The gain, however, is used in the calculation of the transfer-matrix elements [see (5), (6) and (9)], which are in turn used to compute the optical intensity distribution. To account for this nonlinear behavior, we solve for the gain and intensity distributions using the following iterative approach.

1) A first-order approximation of the internal-intensity distribution is calculated assuming no intensity dependence of the gain.
2) An approximate value of the intensity within each subsection is calculated by averaging the intensity values at both ends of the subsection.
3) The modal gain for each subsection is recalculated using (13) and the intensity values from Step 2.
4) New intensity-modified transfer matrices are calculated for the amplifier by using the gain from Step 3 and (5), (6), and (9).
5) The internal-intensity distribution is recalculated using the transfer matrices from Step 4.
6) Steps 2–5 are repeated until the deviation from the previous intensity distribution is smaller than the desired error. We find that 15 iterations are enough to obtain less than 0.1% deviation in the optical intensity.

For regions of optical bistability, the initial field used to compute the internal-intensity distribution is not taken to be the input field, since it leads to two stable solutions of the output field. Instead, the intensity computation (Steps 1 and 5 above) begins with an assumed output field and the inverse of each transfer matrix is applied until the input field is reached. This method readily calculates the bistability hysteresis. Since the intensity distribution within the nonuniform device is

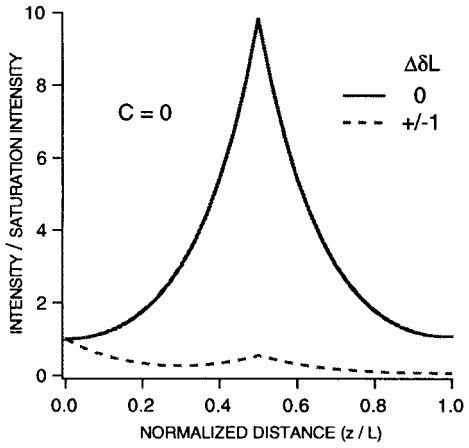

(a)

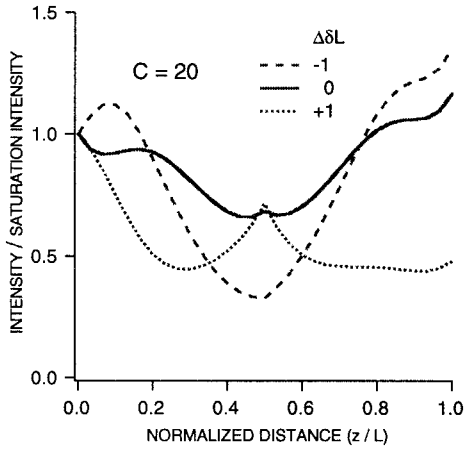

(b)

Fig. 4. (a) The small-signal intensity distribution within a $\lambda/4$ phase-shifted DFB SLA with $\kappa L = 3$, $\alpha = 5$, $\alpha_{\rm int} L = 0$, and $g_o L = 0.6339$ (corresponding to a peak G value of 30 dB) for three values of $\Delta\delta L$. The parameter $\Delta\delta L$ is given by $\Delta\delta L = \delta L - \overline{\delta L}$, where $\overline{\delta L}$ is the value of δL that yields the highest amplifier gain; in this case, $\overline{\delta L} = 1.58$. (b) The small-signal intensity distribution within a linearly chirped, $\lambda/4$ phase-shifted DFB SLA with $\kappa L = 3$, $\alpha = 5$, $\alpha_{\rm int} L = 0$, and $g_o L = 2.4914$ (corresponding to a peak G value of 30 dB) for three values of $\Delta\delta L$ with $\overline{\delta L} = 6.2$.

typically nonuniform, an accurate calculation of the bistability hysteresis requires many values of the internal intensity. However, for some arrangement of grating nonuniformities, it seems possible to flatten the internal intensity completely, so that a single averaged intensity may be used. For the grating nonuniformities considered in this paper, we find that the hysteresis computation converges at about eight values of the internal intensity.

Bistability exists for values of δL less than those corresponding to the transmission peaks. Within this region, a given value of δL supports a range of input intensities that produce three values of the output intensity, the middle of which is unstable. The high bound of this range is the input intensity for which switch-on occurs, and the low-bound corresponds to the switch-off intensity. Starting from a value of δL near the onset of bistability, decreasing δL will increase the bistable region of input intensities and increase the contrast between the top and the bottom of the hysteresis. This is evident in Fig. 5(a), where we plot the hysteresis for the same device parameters as Fig. 2(b). The value of $g_o L$ is chosen to yield an unsaturated peak G value of 30 dB, and δL is decreased from $\delta L = 1.5$ until the switch-on input intensity reaches an upper limit of 1% of the saturation intensity. As apparent from Fig. 5(a), a detuning range of approximately 0.3 δL exists for this region of low-threshold bistable switching. Using typical values of $I_{\rm sat} = 1$ MW/cm^2, $W = 2$ μm, and $d = 0.1$ μm, the required optical power in this low-threshold region is less than 0.1 mW.

The addition of positive linear spatial chirp to the grating of a $\lambda/4$ phase-shifted DFB SLA increases the range of wavelengths that support low-threshold bistable switching for an amplifier driven to provide the same unsaturated peak amplifier gain. This is seen clearly in Fig. 5(b), where we show the bistability hysteresis for a linearly chirped, $\lambda/4$ phase-shifted DFB SLA with $C = 20$. As in Fig. 5(a), the highest value of the δL ($\delta L = 6.0$) is chosen to be near the onset of bistability and δL is decreased until the switch-on input intensity reaches 1% of the saturation intensity. The range of δL values is now 0.9, three times wider than that of the nonchirped case. The contrast is also significantly increased.

These improvements may be understood as follows. The reduction of feedback to the wavelength with the lowest lasing threshold requires the SLA to be pumped at a higher gain to achieve the same unsaturated peak amplifier gain. This additional gain increases the switching contrast. Moreover, a wider range of wavelengths exhibit low-threshold switching because the increased gain raises the intensities at these wavelengths and because the Bragg wavenumber, for which feedback is the greatest, now extends over a range of wavelengths.

Since the transmission spectrum of DFB SLA's shifts with the direct variation of gain (see Figs. 2 and 3), it is possible to tune the bistability hysteresis for a given wavelength. To illustrate this, we first consider a $\lambda/4$ phase-shifted amplifier and choose the value of δL that is 0.3 less than the value for which bistability begins. Fig. 6(a) shows the hysteresis of this amplifier for four values of gain, beginning from the value of $g_o L$ that yields an unsaturated G peak of 30 dB. As seen in the figure, it is possible to select different switching intensities and switching contrasts.

Using the additional degree of freedom provided by gain-tuning, we can compare the bistability characteristics with and without spatial chirp by maintaining a fixed value of δL and varying $g_o L$ (in contrast to Fig. 5, where the opposite was performed). Using the value of δL that is 0.3 less than the value for which bistability begins, the switch-on input intensity is much lower for the case $C = 20$ than for the nonchirped device, if each device is driven to provide a 30-dB unsaturated transmission peak (compare the solid lines of Fig. 6). The switch-on input intensities of the two devices can be set equal by varying the gain of each amplifier. As shown in Fig. 6, approximately equal switch-on intensities exist for the two devices at input intensities just higher than 0.2% of the saturation intensity. In this case, the chirped amplifier is (again) found to have a much larger switching contrast. Another difference between the bistability characteristics is

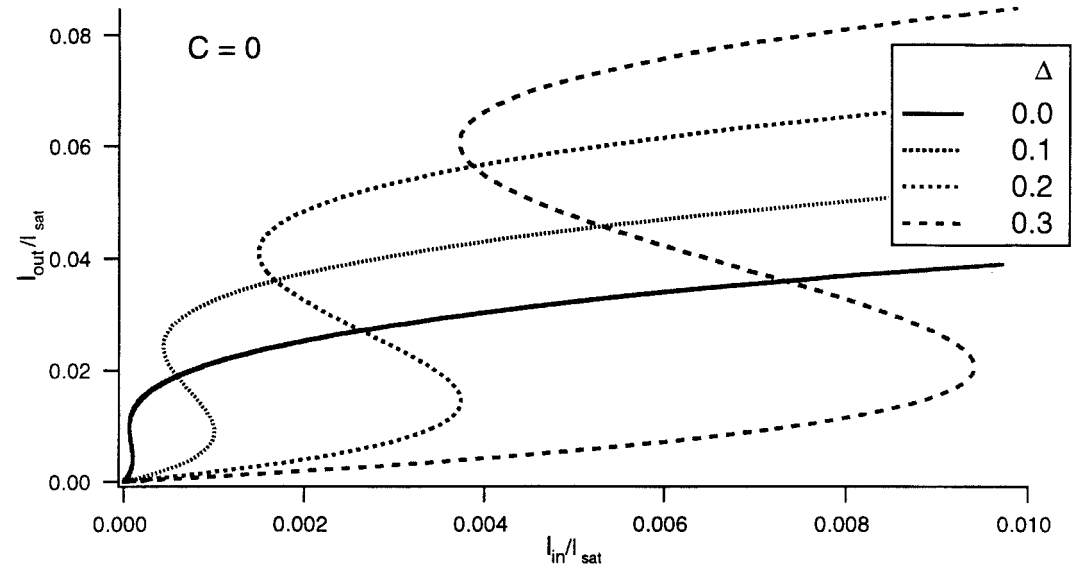

(a)

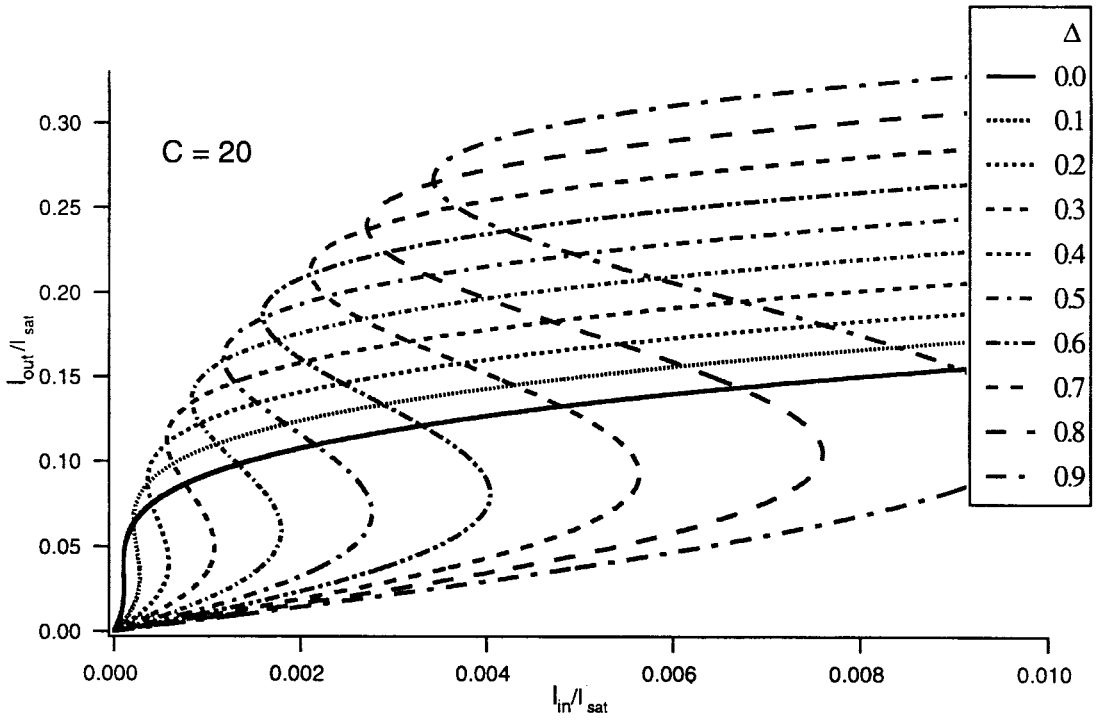

(b)

Fig. 5. (a) The bistability hysteresis for a $\lambda/4$ phase-shifted DFB SLA with $\kappa L = 3$, $\alpha = 5$, $\alpha_{\rm int} L = 0$, and $g_o L = 0.6339$ (corresponding to an unsaturated peak G value of 30 dB) for many values of Δ. The parameter Δ is given by $\Delta = \delta L' - \delta L$, where $\delta L'$ is the value of δL chosen to be near the onset of bistability; in this case, $\delta L' = 1.5$. (b) The bistability hysteresis for a linearly chirped, $\lambda/4$ phase-shifted DFB SLA with $\kappa L = 3$, $\alpha = 5$, $\alpha_{\rm int} L = 0$, and $g_o L = 2.4914$ (corresponding to an unsaturated peak G value of 30 dB) for many values of Δ with $\delta L' = 6.0$.

that the top of the hysteresis is flatter for the chirped case. This behavior can be utilized in bistability-based optical signal regenerators [5] to produce pulses with flatter peaks.

V. Conclusion

In this paper, we presented a TMM capable of simulating optical bistability in DFB SLA's with nonuniform gratings. Computations required a small, initial set of five dimensionless parameters: $\kappa\ell$, $g_o\ell$, $\delta\ell$, $\alpha_{\rm int}\ell$, and α. The linewidth enhancement factor α has been incorporated in a way that takes into account the shift of the transmission spectrum resulting from direct gain variation. This additional degree of freedom allowed us to study the current-induced tuning of the bistability hysteresis (as depicted in Fig. 6). The computation of the bistability characteristics required the calculation of the uneven intensity distribution resulting from grating nonuniformities. We outlined a simple way to perform this computation, including how to account for the nonlinear behavior of gain saturation.

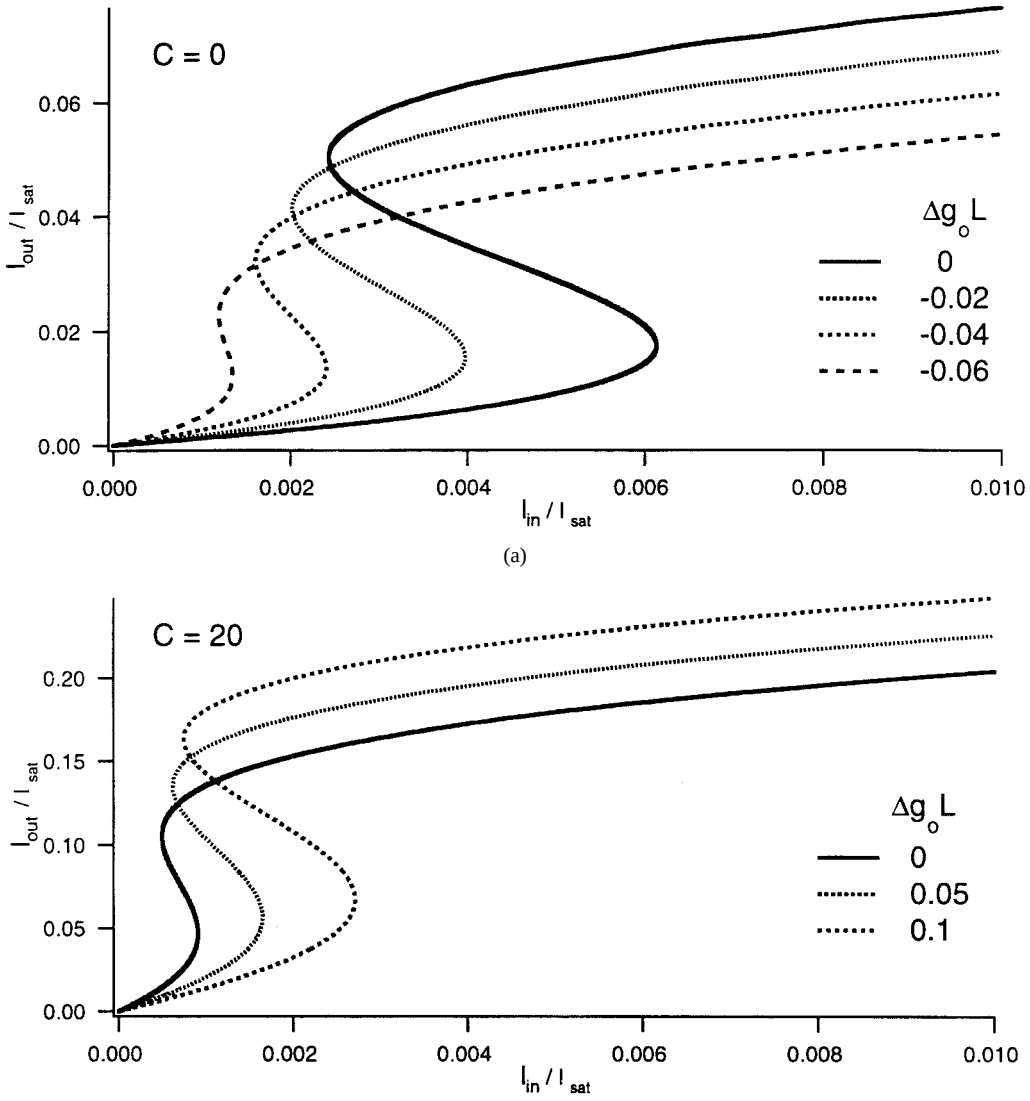

Fig. 6. (a) The bistability hysteresis for a $\lambda/4$ phase-shifted DFB SLA with $\kappa L = 3$, $\alpha = 5$, and $\alpha_{\rm int} L = 0$ as a function of $\Delta g_o L$. The parameter $\Delta g_o L = g_o L - \overline{g_o L}$, where $\overline{g_o L}$ is the value which yields an unsaturated peak G value of 30 dB; in this case $\overline{g_o L} = 0.6339$. The parameter δL is chosen to be 0.3 less than its value at the exact onset of bistability; in this case $\delta L = 1.25$. (b) The bistability hysteresis for a linearly chirped, $\lambda/4$ phase-shifted DFB SLA with $\kappa L = 3$, $\alpha = 5$, and $\alpha_{\rm int} L = 0$ for many values of $\Delta g_o L$ with $\overline{g_o L} = 2.4914$ and $\delta L = 5.73$.

Each nonuniformity considered in this paper increased the number of required parameters by one. The linearly chirped, $\lambda/4$ phase-shifted DFB SLA required a value of the phase shift and a value of the chirp parameter C. For small-signal amplification, we found that linear chirp simultaneously widened the transmission peak and increased the discrimination between transmission peaks of different amplifier gains. Therefore, we believe these devices may find application as demultiplexers for high-capacity (i.e., short pulse) WDM communication systems.

Within the regime of optical bistability, we found that linear chirp extended the spectral range of low-threshold bistable switching for $\lambda/4$ phase-shifted DFB amplifiers driven to yield the same unsaturated peak amplifier gain. Linear chirp also increased the switching contrast and reduced the slope of the top of the bistability hysteresis. In addition, since the active semiconductor transmission spectra can be tuned by adjusting the gain, this novel grating structure provides a tunable, low-threshold bistable amplifier.

In our steady-state analysis, we did not address the switching speed of the DFB SLA. The study of pulse evolution through nonuniform grating amplifiers should also yield interesting behavior; we are currently investigating these topics. In addition, we are also using the TMM to study the effects of nonuniform gratings for specific applications in optical logic, optical communications, and optical signal processing. We believe that the TMM provides a simple and insightful means of studying this unique way of tailoring the bistability characteristics of DFB SLA's.

ACKNOWLEDGMENT

The authors acknowledge fruitful discussions with J. R. Marciante, S. Radic, and G. H. M. van Tartwijk. They would also like to thank the referees for their insightful comments.

REFERENCES

[1] M. J. Adams, H. J. Westlake, and M. J. O'Mahony, "Optical bistability in semiconductor laser amplifiers," in *Optical Nonlinearities and Instabilities in Semiconductors,* H. Haug, Ed. San Diego, CA: Academic Press, 1988, ch. 15.

[2] W. F. Sharfin and M. Dagenais, "High contrast, 1.3 μm optical AND gate with gain," *Appl. Phys. Lett.,* vol. 48, pp. 1510–1512, 1986.

[3] N. Ogasawara and R. Ito, "Static and dynamic properties of nonlinear semiconductor lasers amplifiers," *Jpn. J. Appl. Phys.,* vol. 25, pp. L739–L742, 1986.

[4] K. Inoue, "All-optical flip-flop operation in an optical bistable device using two lights of different frequencies," *Opt. Lett.,* vol. 12, pp. 918–920, 1987.

[5] R. P. Webb, "Error-rate measurements on an all-optically regenerated signal," *Opt. Quantum Electron.,* vol. 19, pp. S57–S60, 1987.

[6] M. Dagenais and W. F. Sharfin, "Bistable diode laser amplifiers in high performance optical communication and optical computing systems," *SPIE Proc.,* vol. 881, pp. 80–91, 1988.

[7] H. Kogelnik, "Filter response of nonuniform almost-periodic structures," *Bell Syst. Tech. J.,* vol. 55, pp. 109–126, 1976.

[8] M. Yamada and K. Sakuda, "Analysis of almost-periodic distributed feedback slab waveguides via a fundamental matrix approach," *Appl. Opt.,* vol. 26, pp. 3474–3478, 1987.

[9] ———, "Adjustable gain and bandwidth light amplifiers in terms of distributed feedback structures," *J. Opt. Soc. Amer. A,* vol. 4, pp. 69–76, 1987.

[10] T. Makino and J. Glinksi, "Transfer matrix analysis of the amplified spontaneous emission of DFB semiconductor laser amplifiers," *IEEE J. Quantum Electron.,* vol. 24, pp. 1507–1518, 1988.

[11] G. P. Agrawal and A. H. Bobeck, "Modeling of distributed feedback semiconductor lasers with axially-varying parameters," *IEEE J. Quantum Electron.,* vol. 24, pp. 2407–2414, 1988.

[12] H. Ghafouri-Shiraz, B. S. K. Lo, and C. Y. J. Chu, "Structural dependence of three-phase-shift distributed feedback semiconductor laser diodes at threshold using the transfer matrix method," *Semicond. Sci. Technol.,* vol. 9, pp. 1126–1132, 1994.

[13] S. Radic, N. George, and G. P. Agrawal, "Analysis of nonuniform nonlinear distributed feedback structures: Generalized transfer matrix method," *IEEE J. Quantum Electron.,* vol. 31, pp. 1326–1336, 1995.

[14] N. Chinone and M. Okai, "Distributed feedback semiconductor lasers," in *Semiconductor Lasers; Past, Present, and Future,* G. P. Agrawal, Ed. New York: AIP Press, 1995, ch. 2.

[15] M. J. Adams and R. Wyatt, "Optical bistability in distributed feedback semiconductor laser amplifiers," *Proc. Inst. Elect. Eng.,* vol. 134, pp. 35–40, 1987.

[16] K. Magari, H. Kawaguchi, K. Oe, and M. Fukuda, "Optical narrow-band filters using optical amplification with distributed feedback," *IEEE J. Quantum Electron.,* vol. 24, pp. 2178–2190, 1988.

[17] R. Hui and A. Sapia, "Nonlinearity difference in the two passbands of a distributed-feedback semiconductor laser amplifier," *Opt. Lett.,* vol. 15, pp. 956–958, 1990.

[18] H. Kogelnik and C. V. Shank, "Coupled-wave theory of distributed feedback lasers," *J. Appl. Phys.,* vol. 43, pp. 2327–2335, 1972.

[19] G. P. Agrawal and N. K. Dutta, *Semiconductor Lasers,* 2nd ed. New York: Van Nostrand Reinhold, 1993.

[20] K. David, J. Buus, and R. G. Baets, "Basic analysis of AR-coated, partly gain-coupled DFB lasers: The standing wave effect," *IEEE J. Quantum Electron.,* vol. 28, pp. 427–433, 1992.

[21] M. J. Adams, H. J. Westlake, M. J. O'Mahony, and I. D. Henning, "A comparison of active and passive optical bistability in semiconductors," *IEEE J. Quantum Electron.,* vol. QE-21, pp. 1498–1504, 1985.

[22] H. Kawaguchi, K. Magari, K. Oe, Y. Noguchi, Y. Nakano, and G. Motosugi, "Optical frequency-selective amplification in a distributed feedback type semiconductor laser amplifier," *Appl. Phys. Lett.,* vol. 50, pp. 66–67, 1987.

[23] K. Magari, H. Kawaguchi, K. Oe, Y. Nakano, and M. Fukuda, "Optical signal selection with a constant gain and a gain bandwidth by a multielectrode distributed feedback laser amplifier," *Appl. Phys. Lett.,* vol. 51, pp. 1974–1976, 1987.

[24] T. Numai, M. Fujiwara, N. Shimosaka, K. Kaede, M. Nishio, S. Suzuki, and I. Mito, "1.5 μm λ/4-shifted DFB LD filter and 100 Mbit/s two-channel wavelength signal switching," *Electron. Lett.,* vol. 24, pp. 236–237, 1988.

[25] H. Hillmer, K. Magari, and Y. Suzuki, "Chirped gratings for DFB laser diodes using bent waveguides," *IEEE Photon. Technol. Lett.,* vol. 5, pp. 10–12, 1993.

[26] H. Hillmer, A. Grabmaier, S. Hansmann, H.-L. Zhu, H. Burkhard, and K. Magari, "Tailored DFB laser properties by individually chirped gratings using bent waveguides," *IEEE J. Select. Topics Quantum Electron.,* vol. 1, pp. 356–362, 1995.

[27] H. G. Winful, J. H. Marburger, and E. Garmire, "Theory of bistability in nonlinear distributed feedback structures," *Appl. Phys. Lett.,* vol. 35, pp. 379–381, 1979.

Drew N. Maywar was born in Port Huron, MI, on March 1, 1970. He received the B.S. degree in optics and the B.A. degree (with honors) in religion in 1993 and the M.S. degree in optics in 1997, all from the University of Rochester, Rochester, NY. He is currently pursuing the Ph.D. degree in optics at the same university.

In 1991, he spent a year at the Center for Japanese Studies, Nanzan University, Japan. From 1993 to 1994, he was a Fulbright scholar at Osaka University's Institute of Laser Engineering, where he worked on the temperature dependence of gain in Nd:glass laser amplifiers. His current research interests are optical switching and distributed feedback, active semiconductor, and fiber devices.

Govind P. Agrawal (M'83–SM'86–F'96), for photograph and biography, see p. 468 of the March 1997 issue of this JOURNAL.